Dynamics of nonlinear Schrödinger breathers in a potential trap

B. A. Malomed,[1,2,3] N. N. Rosanov,[3,4,5] and S. V. Fedorov[3]

[1]*Department of Physical Electronics, School of Electrical Engineering, Faculty of Engineering, Tel Aviv University,*
P.O.B. 39040, Ramat Aviv, Tel Aviv, Israel
[2]*Center for Light-Matter Interaction, Tel Aviv University, P.O.B. 39040, Ramat Aviv, Tel Aviv, Israel*
[3]*Saint Petersburg National Research University of Information Technologies, Mechanics and Optics (ITMO University),*
197101 Saint Petersburg, Russia
[4]*Vavilov State Optical Institute, 199053 Saint Petersburg, Russia*
[5]*Ioffe Physical-Technical Institute, Russian Academy of Sciences, 194021 Saint Petersburg, Russia*

We consider the evolution of the 2-soliton (breather) of the nonlinear Schrödinger equation on a semi-infinite line with the zero boundary condition and a linear potential, which corresponds to the gravity field in the presence of a hard floor. This setting can be implemented in atomic Bose-Einstein condensates, and in a nonlinear planar waveguide in optics. In the absence of the gravity, repulsion of the breather from the floor leads to its splitting into constituent fundamental solitons, if the initial distance from the floor is smaller than a critical value; otherwise, the moving breather persists. In the presence of gravity, the breather always splits into a pair of "co-hopping" fundamental solitons, which may be frequency locked in the form of a *quasi-breather*, or unlocked, forming an incoherent *pseudo-breather*. Some essential results are obtained in an analytical form, in addition to the systematic numerical investigation.

I. INTRODUCTION

The nonlinear Schrödinger (NLS) equation is a fundamental model for a broad class of physical settings combining weak nonlinearity and weak linear dispersion or diffraction [1]. It is commonly known that, in the absence of additional terms, the NLS equations with either self-focusing or defocusing sign of the nonlinearity are integrable, the former one giving rise to exact single- and multi-soliton solutions. An essential extension of the concept of fundamental single-soliton states is provided by the class of higher-order n-solitons ($n = 2,3,4,\dots$), which are produced, as exact solutions, by the input in the form of the fundamental soliton multiplied by integer n [2]. Alternatively, one can create a fundamental soliton, corresponding to $n = 1$, and apply a *quench* of the nonlinearity strength, making it stronger by a factor of n^2 [3–9], which may be implemented, in particular, in atomic Bose-Einstein condensates (BECs) by means of the Feshbach resonance [10]. Higher-order solitons are bound states of n fundamental ones with unequal amplitudes, whose binding energy is exactly zero (therefore, they are subject to weak splitting instability). They perform periodic oscillations (at a frequency which does not depend on n), hence the name of "breathers." In particular, the 2- and 3-solitons are built as bound states of fundamental solitons with ratios of amplitudes and norms 3 : 1 and 5 : 3 : 1, respectively [2].

In spite of the above-mentioned weak splitting instability, n-solitons, and, first of all, 2-solitons are relevant self-trapped modes, as they are readily generated experimentally, along with fundamental solitons and other varieties of multi-soliton states, in nonlinear optics [11–18] as well as in BEC [19], magnetic media [20], superconductors [21], and in other settings. In particular, a relevant issue is interaction of breathers with local defects and potential walls, as well as dynamics of breathers trapped in potential wells. The latter is the subject of the present work, as concerns the 2-solitons. The interaction with defects (including nonlinear potential barriers or traps, represented by narrow regions carrying strong nonlinearity [22–25]), walls, and potential wells was studied in detail for fundamental bright solitons [26–34], but not for the breathers.

In this work, we address the dynamics of 2-solitons in the framework of the NLS equation for wave function $\psi(z,t)$ on a semi-infinite axis, $z \geqslant 0$, with the zero (reflective) boundary condition (b.c.), $\psi(z = 0) = 0$. The equation, written in the scaled form, includes a linear potential Gz, which represents a constant force:

$$i\psi_t = -(1/2)\psi_{zz} - |\psi|^2\psi + Gz\psi, \qquad (1)$$

the respective Hamiltonian being

$$H = \int_{-\infty}^{+\infty} \left(\frac{1}{2}|\psi_z|^2 dz - \frac{1}{2}|\psi|^4 dz + Gz|\psi|^2 \right) dz. \qquad (2)$$

In addition to the Hamiltonian, Eq. (1) conserves the total norm,

$$N = \int_{-\infty}^{+\infty} |u(z)|^2 dz. \qquad (3)$$

This model directly applies to BEC in a vertically or obliquely placed cigar-shaped (quasi-one-dimensional) trap, under the action of gravity, with the "hard floor" at $z = 0$ provided by a repelling laser sheet [35,36]. With temporal and spatial scales typical of BEC experiments, $t_0 \sim 1$ ms and $z_0 \sim 1$ μm, the value of G corresponding to the vertically placed trap holding atoms of ^{7}Li under the action of the natural gravity field is $G \sim 1$. Below, we consider essentially smaller values, viz., $G = 0.001$, 0.01, and 0.1, which correspond to

oblique placement of the quasi-one-dimensional trap, under small angles with the horizontal direction, $\theta \sim 0.05^\circ$, 0.5°, and 5°, respectively. Alternatively, this setting may be realized under the action of microgravity [37]. Equation (1) with t replaced by the propagation distance models the transmission of optical or terahertz waves in planar nonlinear waveguides, with an edge at $z = 0$, the gravity term representing spatial modulation of the refractive index [18,38]. In this case, the gradient of the refractive index, corresponding to Eq. (1), is $\sim (G/100)\lambda^{-1}$ in physical units, where λ is the carrier wavelength. While this value may be unrealistically high for $G \sim 1$ and a typical optical wavelength, $\lambda \sim 1$ μm, the estimate yields reasonable values for terahertz radiation.

The rest of the paper is organized as follows. In Sec. II, we report some analytical results which predict characteristic features of the 2-soliton's dynamics in the present model. Results of systematic numerical simulations, produced by means of the standard split-step Fourier-transform algorithm, are reported in Sec. III, and the paper is concluded by Sec. IV.

II. ANALYTICAL ESTIMATES

In the absence of b.c. $\psi(z = 0) = 0$ and linear potential Gz, the initial condition $\psi(z, t = 0) = 2\eta \, \text{sech}(\eta z)e^{iVz}$, with arbitrary real constants η and V, gives rise to the exact breather (2-soliton) solution of integrable equation (1), oscillating with frequency

$$\omega_{\text{br}} = 4\eta^2 \qquad (4)$$

and moving with velocity V [2]:

$$\psi_{\text{br}}(z,t) = 4\eta \frac{\cosh\left[3\eta(z - Vt)\right] + 3e^{4i\eta^2 t}\cosh\left[\eta(z - Vt)\right]}{\cosh\left[4\eta(z - Vt)\right] + 4\cosh\left[2\eta(z - Vt)\right] + 3\cos(4\eta^2 t)} \exp[iVz + (i/2)(\eta^2 - V^2)t]. \qquad (5)$$

Note that the breather periodically returns to the initial configuration, with the single central maximum of density $|\psi(z,t)|^2$, at times $t = 2(\pi/\omega_{\text{br}})m$ with integer m, and at other times $t = (\pi/\omega_{\text{br}})(1 + 2m)$ the density profile features small side maxima, separated from the central peak by distance

$$\Delta z \approx \pm 1.32/\eta. \qquad (6)$$

If the b.c. [39,40], or the linear potential [41] are separately added to the NLS equation, these terms do not break its integrability. However, if combined together, they make Eq. (2) a *nonintegrable* model of the potential trap, corresponding to the effective potential

$$U(z) = \begin{cases} Gz & \text{at } z > 0, \\ \infty & \text{at } z < 0. \end{cases} \qquad (7)$$

In terms of the inverse-scattering transform, exact solution (5) is a nonlinear superposition of two fundamental solitons which, in isolation, have the form of

$$\psi_{1,2} = \eta_{1,2} \, \text{sech}(\eta_{1,2}z) \exp\left[(i/2)\left(\eta_{1,2}^2 - V^2\right) + iVz\right], \qquad (8)$$

whose amplitudes

$$\eta_1 = 3\eta, \quad \eta_2 = \eta \qquad (9)$$

are subject to the above-mentioned ratio $\eta_1 : \eta_2 = 3 : 1$, the summary norm of these solitons being equal to the total norm of breather (5): $2(\eta_1 + \eta_2) = 8\eta$ [2]. Because the binding energy of the 2-soliton in the integrable equation is exactly zero, it may fission into a pair of the constituent fundamental solitons (8). In particular, weak time-periodic modulation of the nonlinearity strength with frequency ω gives rise to resonant fission at $\omega = \omega_{\text{br}}$ [42].

The first dynamical situation addressed by means of numerical simulations below, in the absence of gravity ($G = 0$), is to place the center of the 2-soliton with zero velocity at point $z = z_0$, which corresponds to the initial condition

$$\psi(z, t = 0) = 2\eta \, \text{sech}[\eta(z - z_0)], \quad \text{at } z > 0. \qquad (10)$$

The b.c. $\psi(z = 0) = 0$ suggests to replace this input by one combining the actual input with its mirror image placed, with the opposite sign, at $z < 0$ (so that the zero b.c. identically holds), thus considering Eq. (1) (with $G = 0$, for the time being) on the infinite axis, with the extended initial condition

$$\psi(z, t = 0) = A\{\text{sech}\left[\eta(z - z_0)\right] - \text{sech}\left[\eta(z + z_0)\right]\}. \qquad (11)$$

where the common amplitude, A, is taken as a free parameter, to develop the analysis in a more general form.

The repulsive interaction of the actual quasi-soliton input with its negative mirror image pushes the quasi-soliton towards $z \to \infty$, our objective being to predict velocity V which it will thus acquire. To this end, following Ref. [43] (see also Refs. [44] and [26]), we use an effective potential energy of the repulsive interaction, which can be easily found for input (11):

$$U_{\text{int}} = 8A^2\eta \exp(-2\eta z_0), \qquad (12)$$

assuming $\eta z_0 \gg 1$, cf. Ref. [45]. Further, the total kinetic energy of the quasi-soliton, moving with velocity V, and its mirror image moving with velocity $-V$, is $K = NV^2$, taking into account the well-known fact that the effective mass of each term in expression (11) is equal to its norm [26] [see Eq. (3), where the integration is performed separately for each soliton]: $M_{\text{eff}} = 2A^2\eta$. Lastly, the velocity of the established regime of motion is determined by the energy-balance condition, $U_{\text{int}} = K$, i.e.,

$$V = 2 \exp(-\eta z_0). \qquad (13)$$

It is worthwhile to note that the result given by Eq. (13) is general, in the sense that amplitude A cancels out in it, hence the predicted velocity does not depend on the choice of the initial amplitude, while it depends on the width, η^{-1}. Furthermore, this dependence suggests that the repulsion from the mirror image can make the breather unstable against the fission into the constituent fundamental solitons, characterized by different values $\eta_{1,2}$ [see Eq. (9)], as they give rise to different velocities as per Eq. (13).

Another analytical prediction, relevant for the comparison with numerical results reported below, pertains to the effective equilibrium position of quasi-soliton (10) in the presence of gravity, $G > 0$. Indeed, in this case, the last term in Hamiltonian (2) gives rise to the gravity energy, which we take as the sum of the respective terms for the actual quasi-soliton and its mirror image. Combining it with interaction energy (12), we derive the total potential energy:

$$U_{\text{tot}}(z_0) = 8A^2\eta \exp(-2\eta z_0) + 2GA^2\eta z_0, \qquad (14)$$

which translates the underlying trapping energy (7) into the effective potential for the soliton's central coordinate. The equilibrium position coincides with the minimum of energy (14), $dU_{\text{tot}}(z)/dz = 0$, i.e.,

$$z_{\text{equil}}(G) = (2\eta)^{-1}\ln(8\eta/G), \qquad (15)$$

as recently demonstrated in Ref. [45].

III. NUMERICAL RESULTS

A. Zero-gravity case

As mentioned above, simulations of Eq. (1) with b.c. $\psi(z = 0) = 0$ and input (10) were first run without gravity, $G = 0$, to identify effects of the interaction of the initial breather with its mirror image. The results are displayed here for $\eta = 1.504$, which is chosen for convenience of the presentation (the scaling invariance of the model with $G = 0$ makes all the values of η mutually equivalent).

An essential finding is the existence of a critical value of the initial position of the 2-soliton's center,

$$(z_0)_{\text{cr}} \approx 5.194, \qquad (16)$$

such that, as conjectured above on the basis of Eq. (13), the 2-soliton, originally placed with zero velocity at $z_0 < (z_0)_{\text{cr}}$, splits into two fundamental solitons, precisely with the expected amplitudes predicted by Eq. (9), as shown in the panel of Fig. 1 pertaining to $z_0 = 5.193$. The released fundamental solitons slowly separate, moving towards $z \to \infty$. In the case of $5.194 \leqslant z_0 < 5.4$, the breather survives in the form of a moving oscillatory bound state, as in this case the attraction between the constituent fundamental solitons is sufficient to overcome the splitting factor, which attenuates exponentially with the increase of z_0, as per Eq. (13). The velocity of the moving bound state is accurately predicted by Eq. (13) [see Fig. 2(b) below], while its oscillation frequency is much lower than the standard value given by Eq. (4), as seen in panels of Fig. 1 pertaining to $z_0 = 5.194$, 5.2, and 5.25. Eventually, at $z_0 \geqslant 5.4$, the moving breather restores the standard oscillation frequency (4), as shown in the panels of 1 corresponding to $z = 5.4$.

Note that, in the interval of $5.194 \leqslant z_0 < 5.4$, the breather is different from exact solution (5), as it exhibits a single side maximum oscillating around the central peak, unlike the pair of symmetric side maxima in solution (5), whose positions are given by Eq. (6). Such generalized spatially asymmetric solutions for NLS breathers are known too [46]. The usual symmetric shape is nearly restored at $z_0 \geqslant 5.4$. In particular, the largest distance between the side maxima in the panel of Fig. 1 pertaining to $z_0 = 5.4$ coincides with the double value given by Eq. (6).

Systematically collected results of the simulations are summarized in Fig. 2. Naturally, both the period of oscillations, T, and the oscillation amplitude, Δz, diverge as the breather is approaching the fission point, $z_0 - 5.193 \to +0$. Concerning
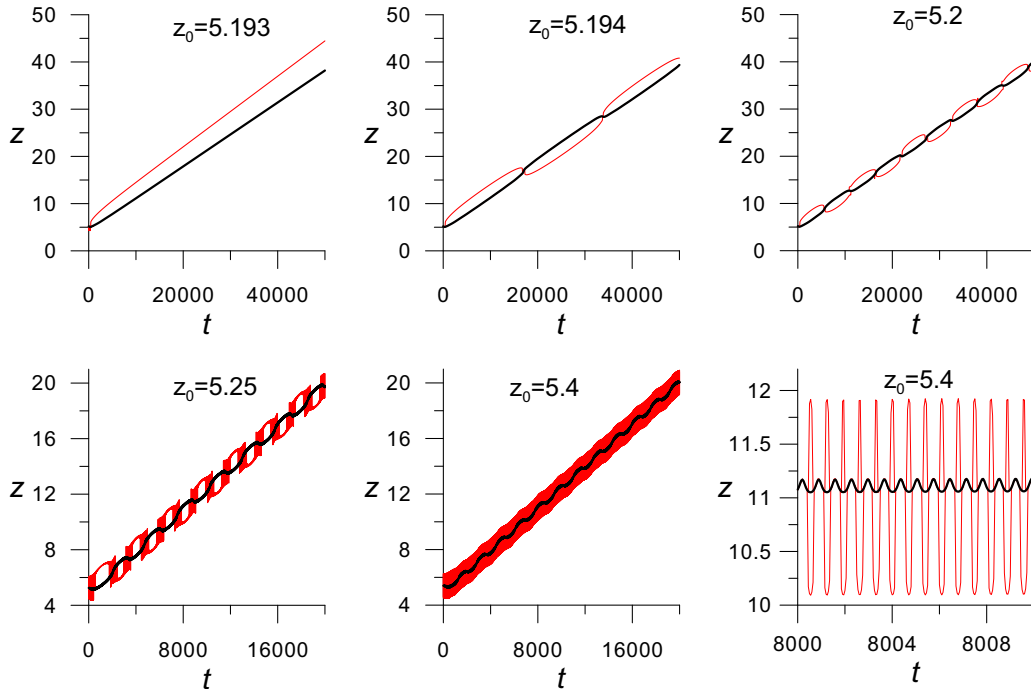

FIG. 1. The motion of local maxima of density $|\psi(z,t)|^2$, as produced by numerical solutions of Eq. (1) in the absence of gravity ($G = 0$) with input (10) taken at different values of z_0, which are indicated in individual panels (the last panel displays details of the high-frequency oscillations for $z_0 = 5.4$). Black and red lines depict, severally, the higher central maximum and lower side ones.
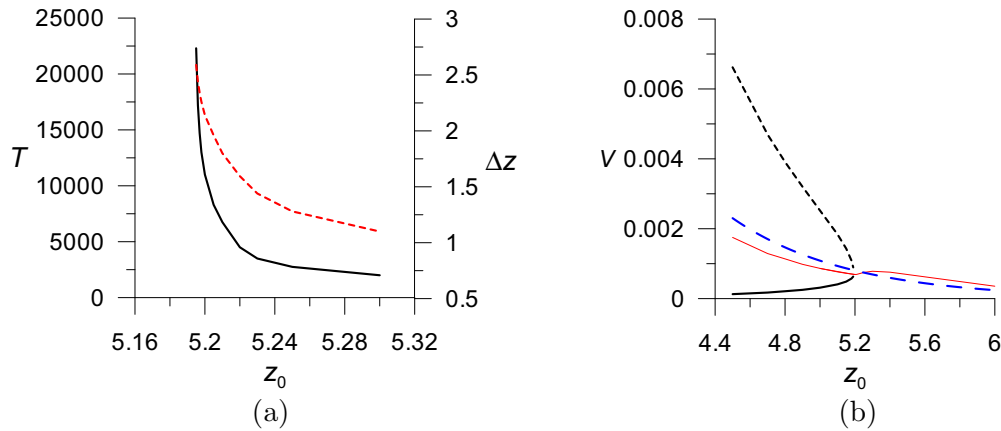
FIG. 2. (a) The solid black and dashed red lines show, severally, period T of oscillations of the moving bound state and the respective largest distance Δz between the higher density maximum and the smaller one oscillating around it, see Fig. 1, vs the initial position z_0 in the absence of gravity, $G = 0$. (b) Solid and dashed black lines show, respectively, velocities V of motion of the heavy and light fundamental solitons, in the case of the fission of the 2-soliton, i.e., at $z < 5.193$. The red line is the velocity of the motion of the center of mass, for the split and unsplit states alike. The dashed blue line shows the analytical prediction given by Eq. (13) for the velocity of the unsplit 2-soliton, or for the center-of-mass velocity of the pair of separating solitons.

the velocity, it is worthwhile to mention that the analytical prediction given by Eq. (13) is quite accurate both for the unsplit breather and for the center of mass of the split pair of the fundamental solitons; see the blue dashed curve in panel 2(b).

Lastly, the above-mentioned scaling invariance of Eq. (1) with $G = 0$ implies that, for other values of amplitude η of input (10) (recall the above results are displayed for fixed $\eta = 1.504$), the critical input's coordinate, $(z_0)_{cr}$, can be obtained from the above value (16), multiplying it by $(1.504/\eta)^2$.

B. Formation of quasi- and pseudo-breathers in the presence of gravity

If the gravity field is included in Eq. (1), the original breather always suffers fission, but the gravity does not allow the splinters (fundamental constituent solitons), or the breather as a whole, to escape, unlike the case of $G = 0$ considered above. As a result, the system relaxes into a dynamical state which may be classified either as a "quasi-breather," originating from the input with z_0 relatively small, or as a "pseudo-breather," for larger z_0. In the former case, the fundamental solitons periodically collide with relatively small velocities, which

makes the effective interaction between them strong enough to frequency-lock their oscillatory ("co-hopping") motion, as seen in panels pertaining to $z_0 = 1.9$ and 2.6 in Fig. 3, with the ratios of the locked frequencies of the heavy and light solitons being, respectively, 3 : 1 and 1 : 1. On the other hand, the dynamical regime originating from larger values of z_0, such as $z_0 = 5.0$ in Fig. 3, leads to collisions at relatively large velocities, which attenuates the effective interaction, and prevents the establishment of the frequency-locked regime. Instead, a quasi-random pseudo-breather dynamical state is observed in the latter case, "pseudo" implying the absence of coherence between the motion of the two fundamental solitons. A sequence of elastic collisions between the heavy and light solitons in the latter case is illustrated by Fig. 4 (individual collisions look similar in the frequency-locked quasi-breather regime).

Finally, characteristics of the "co-hopping" regimes, namely, the largest distance of the center-of-mass coordinate of the set of two solitons, z_{max}, from the system's edge ($z = 0$), and the largest separation between the solitons, δz_{max}, are summarized in Fig. 5. In particular, minima of dependences $z_{max}(z_0)$ can be readily predicted as the location of the potential
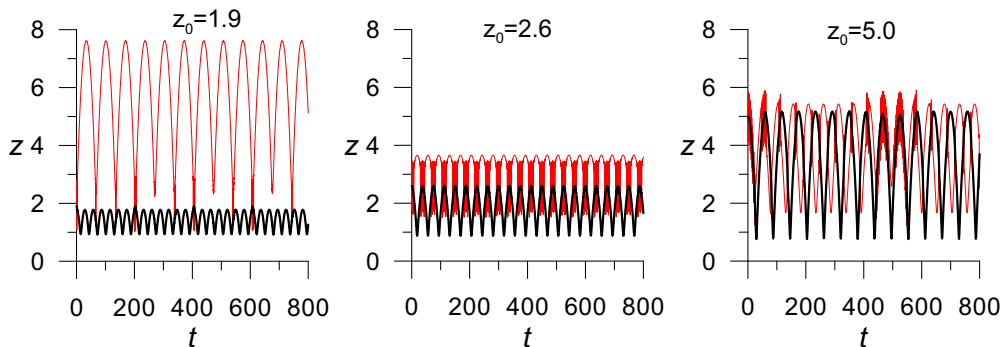

FIG. 3. Black and red lines depict the motion of heavy and light fundamental solitons, as produced by the fission of the 2-soliton input(10) with values of z_0 indicated in the panels, in the presence of gravity with strength $G = 0.01$.
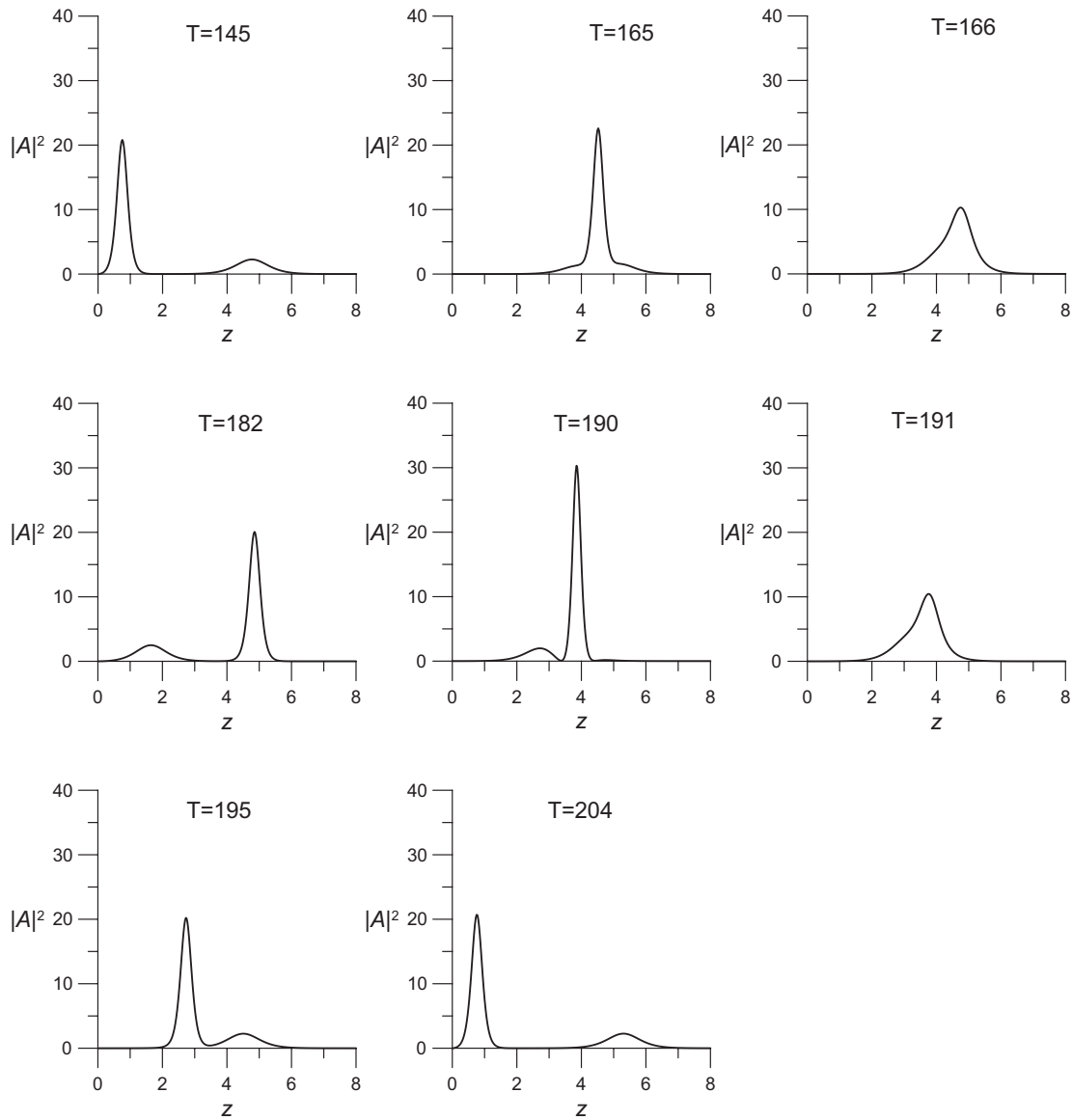
FIG. 4. A set of snapshots corresponding to values of time (T) indicated in panels, which illustrate the dynamical regime of the "pseudo-breather" type, observed at $G = 0.01$ and $z_0 = 5$.
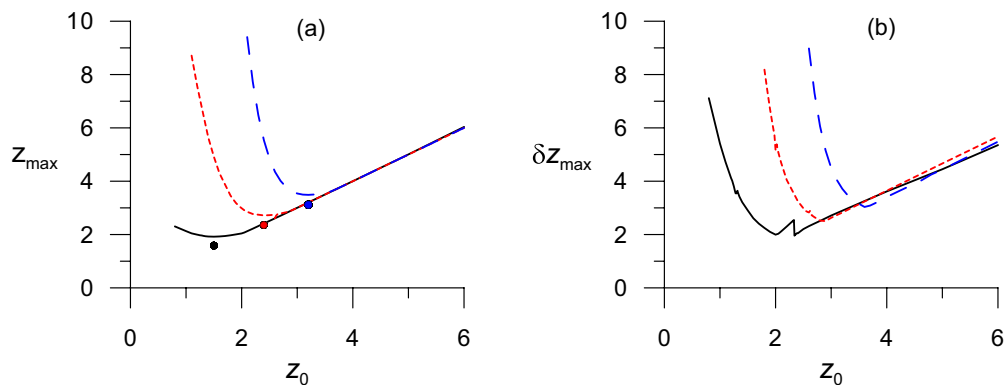

FIG. 5. (a) The largest separation between the center of mass of the two "co-hopping" solitons and the "hard floor" ($z = 0$) vs the initial center-of-mass coordinate, z_0 [see Eq. (10)]. (b) The largest separation between the two solitons, δz_{max}, vs z_0. In both panels, black, red, and blue curves pertain to gravity strengths $G = 0.1$, 0.01, and 0.001, respectively. In (a), dots of the same colors depict respective positions of the analytically predicted potential minima given by Eq. (15).

minimum, z_{equil}, given by Eq. (15) for the same η as in unsplit input (10). Indeed, for $z_0 = z_{\text{equil}}$ the fission of the input is expected to be minimal, while for $z_0 \neq z_{\text{equil}}$ strong fission gives rise to large-amplitude oscillations of the constituent solitons, leading to larger values of z_{max}. Thus, for the values of G, which are represented in Fig. 5, and $\eta = 1.504$ adopted here, Eq. (15) yields $z_{\text{equil}}(G = 0.1) \approx 1.59$, $z_{\text{equil}}(G = 0.01) \approx 2.36$, $z_{\text{equil}}(G = 0.001) \approx 3.12$. These values are shown by dots with coordinates $z_0 = z_{\text{max}} = z_{\text{equil}}(G)$ in Fig. 5(a), being, indeed, quite close to values of z_0 at which the three curves feature their minima.

Lastly, small "notches" observed on the curves in Fig. 5(b) may be explained by effects of the emission of radiation from the moving solitons. Detailed analysis of these weak features is beyond the scope of the present paper.

IV. CONCLUSION

Along with fundamental solitons, breathers, i.e., 2-solitons, have drawn much interest as collective excitations in diverse physical settings modeled by the NLS equation. Here, we have addressed dynamics of breathers in the semi-infinite system with a reflecting edge ("hard floor") and the linear potential, which represents gravity or a similar effective field, in atomic BECs and nonlinear optical waveguides. In the absence of the

gravity, the repulsion of the 2-soliton from its mirror image causes its splitting in two constituent fundamental solitons, with the ratio of norms and amplitudes 3 : 1, if the initial distance of the 2-soliton from the edge is smaller than a critical value; otherwise, it moves away from the edge in the form of a persistent breather. Inclusion of gravity always causes fission of the breather into the same pair of fundamental solitons. They feature "co-hopping" motion, in which they may be frequency-locked into a coherent quasi-breather, or remain in the form of an incoherent pseudo-breather. In addition to the systematic numerical simulations, basic characteristics of the considered dynamical regimes were predicted analytically, with the help of the effective potential for the 2-soliton input.

As an extension of the present analysis, it may be interesting to develop it for 3-solitons. A challenging issue is a possibility of the consideration of multiple solitons in the quantum NLS model, cf. Refs. [8,47–50].

[1] V. E. Zakharov, S. V. Manakov, S. P. Novikov, and L. P. Pitaevskii, *Theory of Solitons* (Nauka, Moscow, 1980); English translation: Consultants Bureau, New York, 1984.

[2] J. Satsuma and N. Yajima, Initial value problems of one-dimensional self-modulation of nonlinear waves in dispersive media, Suppl. Prog. Theor. Phys. **55**, 284 (1974).

[3] S. Mondal, K. Sengupta, and D. Sen, Theory of defect production in nonlinear quench across a quantum critical point, Phys. Rev. B **79**, 045128 (2009).

[4] M. Kormos, M. Collura, and P. Calabrese, Analytic results for a quantum quench from free to hard-core one-dimensional bosons, Phys. Rev. A **89**, 013609 (2014).

[5] P.-E. Larre and I. Carusotto, Propagation of a quantum fluid of light in a cavityless nonlinear optical medium: General theory and response to quantum quenches, Phys. Rev. A **92**, 043802 (2015).

[6] L. Piroli, P. Calabrese, and F. H. L. Essler, Quantum quenches to the attractive one-dimensional Bose gas: Exact results, SciPost Phys. **1**, 001 (2016).

[7] J.-S. Caux, The quench action, J. Stat. Mech.: Theory Exp. (2016) 064006.

[8] V. A. Yurovsky, B. A. Malomed, R. G. Hulet, and M. Olshanii, Dissociation of One-Dimensional Matter-Wave Breathers due to Quantum Many-Body Effects, Phys. Rev. Lett. **119**, 220401 (2017).

[9] J. Golde, J. Ruhl, B. A. Malomed, M. Olshanii, and V. Dunjko, Metastability versus collapse following a quench in attractive Bose-Einstein condensates, Phys. Rev. A (to be published).

[10] C. Chin, R. Grimm, P. Julienne, and E. Tiesinga, Feshbach resonances in ultracold gases, Rev. Mod. Phys. **82**, 1225 (2010).

[11] L. F. Mollenauer, R. H. Stolen, and J. P. Gordon, Experimental Observation of Picosecond Pulse Narrowing and Solitons in Optical Fibers, Phys. Rev. Lett. **45**, 1095 (1980).

[12] K. Tai, A. Hasegawa, and N. Bekki, Fission of optical solitons induced by stimulated Raman effect, Opt. Lett. **13**, 392 (1988).

[13] M. Erkintalo, K. Hammani, B. Kibler, C. Finot, N. Akhmediev, J. M. Dudley, and G. Genty, Higher-Order Modulation Instability in Nonlinear Fiber Optics, Phys. Rev. Lett. **107**, 253901 (2011).

[14] T. Cheng, X. Xue, L. Liu, T. Suzuki, and Y. Ohishi, Experimental observation of mid-infrared higher-order soliton fission in a tapered tellurite microstructured optical fiber, Jpn. J. Appl. Phys. **55**, 060302 (2016).

[15] M. Yu, J. K. Jang, Y. Okawachi, A. G. Griffith, K. Luke, S. A. Miller, X. Ji, M. Lipson, and A. L. Gaeta, Breather soliton dynamics in microresonators, Nat. Commun. **8**, 14569 (2016).

[16] H. R. Guo, E. Lucas, M. H. P. Pfeiffer, M. Karpov, M. Anderson, J. Q. Liu, M. Geiselmann, J. D. Jost, and T. J. Kippenberg, Intermode Breather Solitons in Optical Microresonators, Phys. Rev. X **7**, 041055 (2017).

[17] G. P. Agrawal, *Nonlinear Fiber Optics* (Academic Press, San Diego, 1995).

[18] Y. S. Kivshar and G. P. Agrawal, *Optical Solitons: From Fibers to Photonic Crystals* (Academic Press, San Diego, 2003).

[19] P. J. Everitt, M. A. Sooriyabandara, G. D. McDonald, K. S. Hardman, C. Quinlivan, P. Manju, P. Wigley, J. E. Debs, J. D. Close, C. C. N. Kuhn, and N. P. Robins, Observation of breathers in an attractive Bose gas, arXiv:1509.06844.

[20] S. M. Mohseni, S. R. Sani, J. Persson, T. N. A. Nguyen, S. Chung, Ye. Pogoryelov, P. K. Muduli, E. Iacocca, A. Eklund, R. K. Dumas, S. Bonetti, A. Deac, M. A. Hoefer, and J. Akerman,

Spin torque-generated magnetic droplet solitons, Science **339**, 1295 (2013).

[21] A. Dienst, E. Casandruc, D. Fausti, L. Zhang, M. Eckstein, M. Hoffmann, V. Khanna, N. Dean, M. Gensch, S. Winnerl, W. Seidel, S. Pyon, T. Takayama, H. Takagi, and A. Cavalleri, Optical excitation of Josephson plasma solitons in a cuprate superconductor, Nat. Mater. **12**, 535 (2013).

[22] M. T. Primatarowa, K. T. Stoychev, and R. S. Kamburova, Interaction of solitons with extended nonlinear defects, Phys. Rev. E **72**, 036608 (2005).

[23] O. Maor, N. Dror, and B. A. Malomed, Holding spatial solitons in a pumped cavity with the help of nonlinear potentials, Opt. Lett. **38**, 5454 (2013).

[24] N. V. Hung, M. Trippenbach, E. Infeld, and B. A. Malomed, Spatial control of the competition between self-focusing and defocusing nonlinearities in one- and two-dimensional systems, Phys. Rev. A **90**, 023841 (2014).

[25] H. Sakaguchi and B. A. Malomed, Matter-wave soliton interferometer based on a nonlinear splitter, New J. Phys. **18**, 025020 (2016).

[26] Y. S. Kivshar and B. A. Malomed, Dynamics of solitons in nearly integrable systems, Rev. Mod. Phys. **61**, 763 (1989).

[27] M. M. Bogdan, A. S. Kovalev, and I. V. Gerasimchuk, Dynamics and stability of localized modes in nonlinear media with point defects, Low Temp. Phys. **23**, 145 (1997).

[28] R. H. Goodman, P. J. Holmes, and M. I. Weinstein, Strong NLS soliton-defect interactions, Physica D **192**, 215 (2004).

[29] K. T. Stoychev, M. T. Primatarowa, and R. S. Kamburova, Resonant scattering of nonlinear Schrödinger solitons from potential wells, Phys. Rev. E **70**, 066622 (2004).

[30] E. Corrigan and C. Zambon, Jump-defects in the nonlinear Schrödinger model and other non-relativistic field theories, Nonlinearity **19**, 1447 (2006); S. A. Sekh, Bouncing dynamics of Bose–Einstein condensates under the effects of gravity, Phys. Lett. A **381**, 852 (2017).

[31] W. Z. Chen, L. Lu, and Y. F. Zhu, Influence of impurities on hydrodynamic solitons, Phys. Rev. E **71**, 036622 (2005).

[32] A. Alberucci, G. Assanto, A. A. Minzoni, and N. F. Smyth, Scattering of reorientational optical solitary waves at dielectric perturbations, Phys. Rev. A **85**, 013804 (2012).

[33] A. L. Marchant, T. P. Billam, T. P. Wiles, M. M. H. Yu, S. A. Gardiner, and S. L. Cornish, Controlled formation and reflection of a bright solitary matter-wave, Nat. Commun. **4**, 1865 (2013).

[34] F. Genoud, B. A. Malomed, and R. M. Weishäupl, Stable NLS solitons in a cubic-quintic medium with a delta-function potential, Nonlinear Anal. **133**, 28 (2016).

[35] B. D. Esry, C. H. Greene, J. P. Burke, and J. L. Bonn, Hartree-Fock Theory for Double Condensates, Phys. Rev. Lett. **78**, 3594 (1997).

[36] B. P. Anderson and M. A. Kasevich, Macroscopic quantum interference from atomic tunnel arrays, Science **282**, 1686 (1998).

[37] T. van Zoest, N. Gaaloul, Y. Singh, H. Ahlers, W. Herr, S. T. Seidel, W. Ertmer, E. Rasel, M. Eckart, E. Kajari, S. Arnold, G. Nandi, W. P. Schleich, R. Walser, A. Vogel, K. Sengstock, K. Bongs, W. Lewoczko-Adamczyk, M. Schiemangk, T. Schuldt, A. Peters, T. Konemann, H. Muntinga, C. Lämmerzahl, H. Dittus, T. Steinmetz, T. W. Hansch, and J. Reichel, Bose-Einstein condensation in microgravity, Science **328**, 1540 (2010).

[38] A. D. Boardman, P. Egan, L. Velasco, and N. King, Control of planar nonlinear guided waves and spatial solitons with a left-handed medium, J. Opt. A: Pure Appl. Phys. **7**, S57 (2005).

[39] A. S. Fokas and A. R. Its, The nonlinear Schrödinger equation on the interval, J. Phys. A: Math. Gen. **37**, 6091 (2004).

[40] A. Degasperis, S. V. Manakov, and P. M. Santini, Integrable and nonintegrable initial boundary value problems for soliton equations, J. Nonlin. Math. Phys. **12**, 228 (2005).

[41] H.-H. Chen and C.-S. Liu, Solitons in Nonuniform Media, Phys. Rev. Lett. **37**, 693 (1976).

[42] H. Sakaguchi and B. A. Malomed, Resonant nonlinearity management for nonlinear Schrödinger solitons, Phys. Rev. E **70**, 066613 (2004).

[43] B. A. Malomed, Potential of interaction between two- and three-dimensional solitons, Phys. Rev. E **58**, 7928 (1998).

[44] V. I. Karpman and V. V. Solov'ev, A perturbation approach to the two-soliton systems, Physica D **3**, 487 (1981).

[45] N. V. Vysotina and N. N. Rosanov, Levitating soliton of the Bose-Einstein condensate, Zh. Eksp. Teor. Fiz. **123**, 51 (2016).

[46] J. P. Gordon, Interaction forces among solitons in optical fibers, Opt. Lett. **8**, 596 (1983).

[47] A. I. Streltsov, O. E. Alon, and L. S. Cederbaum, Formation and Dynamics of Many-Boson Fragmented States in One-Dimensional Attractive Ultracold Gases, Phys. Rev. Lett. **100**, 130401 (2008).

[48] P. Drummond and S. Chaturvedi, Quantum simulations in phase-space: from quantum optics to ultra-cold physics, Phys. Scr. **91**, 073007 (2016).

[49] C. Weiss and L. D. Carr, Higher-order quantum bright solitons in Bose-Einstein condensates show truly quantum emergent behavior, arXiv:1612.05545.

[50] B. Opanchuk and P. D. Drummond, One-dimensional Bose gas dynamics: Breather relaxation, Phys. Rev. A **96**, 053628 (2017).